High-Pressure, Molecular Weight-Dependent Behavior of (Co)polymer–Solvent Mixtures: Experiments and Modeling

Sang-Ho Lee, Minna A. LoStracco, and Mark A. McHugh*

Department of Chemical Engineering, Johns Hopkins University, Baltimore, Maryland 21218

Received October 28, 1993; Revised Manuscript Received May 25, 1994®

ABSTRACT: Cloud-point data as a function of polymer molecular weight are presented for polyethylene (PE)–dimethyl ether (DME) and poly(ethylene-*co*-methyl acrylate) (35 mol % acrylate) (EMA)–butane mixtures to temperatures of 210 °C and pressures of 2700 bar. The cloud-point curves for PE–DME, at temperatures below ~125 °C, and EMA–butane, at temperatures below ~150 °C, order with respect to the weight average molecular weight. The cloud-point behaviors for these two systems along with the poly(ethylene-*co*-acrylic acid) (4.1 mol % acid) (EAA)–butene system are modeled with the statistical associating fluid theory (SAFT). For each system, a constant value of the binary interaction parameter, k_{ij}, is fit to the parent–solvent cloud-point curve and is used in subsequent calculations. For the EAA system, values for the pure component energy of acid dimerization and the volume of association are obtained from literature spectroscopic data. The SAFT equation, with k_{ij} = 0.0405, can only predict the correct qualitative trends observed for the effect of molecular weight on the PE–DME system probably because SAFT does not account for polar DME–DME interactions. A quantitative fit of the EMA–butane system is obtained with k_{ij} = 0.026 and a slightly adjusted value of the nonspecific interaction energy for EMA. The calculations for the EAA–butene system with k_{ij} = −0.020 are in good agreement with experimental data.

Introduction

The physical properties of acid copolymers and their solutions have been extensively investigated with X-ray diffraction, IR spectroscopy, dynamic-mechanical measurements, differential scanning calorimetry, and viscometry. MacKnight and colleagues[1,2] demonstrated that acrylic acid groups in the backbone of poly(ethylene-*co*-acrylic acid) primarily form dimers at room temperature and that dimer formation decreases substantially at temperatures above 160 °C. Otocka and Kwei[3] showed that the enthalpy of acrylic acid dimerization of the repeat units in the backbone of the copolymer, ~11.5 kcal/mol of dimer, is almost identical with the value for the dimerization of low molecular weight acids in a nonpolar solvent.[4] Longworth and Morawetz[5] found that the enthalpy of hydrogen bonding of methacrylic acid groups in poly(styrene-*co*-methacrylic acid) is similar to that for pivalic acid, the monomer analog for the methacrylic acid repeat unit.

Interestingly, Chang and Morawetz[6] argue that methacrylic acid repeat units in poly(styrene-*co*-methacrylic acid) (SMAA) preferentially form intrapolymer hydrogen-bonded acid dimers at 30 °C if the acid content is below ~5 mol %. Their conclusion about intra versus interpolymer hydrogen bonding is based on the spectroscopic data presented in Figure 1 that compares the extent of hydrogen bonding of pivalic acid to that of methacrylic acid (MAA) in the backbone of SMAA. The concentration of pivalic acid monomers drops appreciably with increasing acid concentration in solution. In contrast, for each SMAA copolymer, the concentration of MAA monomer remains essentially constant, regardless of the concentration of copolymer in solution up to about 10 wt %. They conclude that hydrogen bonding between acid segments depends more on the acid content in the copolymer rather than on the overall copolymer concentration in solution.[6-8] Chang and Morawetz[6] also present osmometry data that show

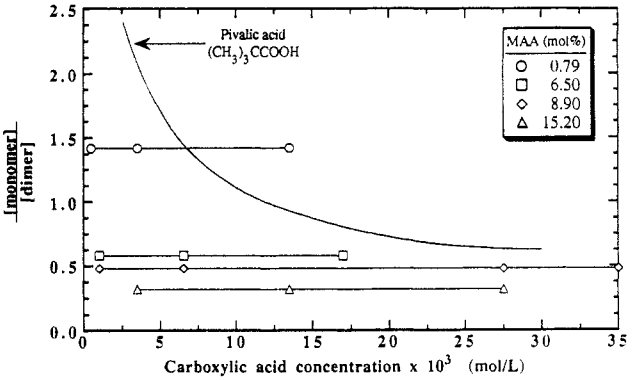

Figure 1. Carboxyl association of pivalic acid and styrene–methacrylic acid copolymer in tetrachloroethane at 29.6 °C.[6] The [monomer]/[dimer] ratio is determined from the optical density at wavelengths corresponding to free and dimerized carboxyl groups.

that the ratio of the "apparent" to "true" molecular weight of SMAA is less than 1.2 for copolymers with less than ~5 mol % acid content. For SMMA with a higher acid content the ratio of the apparent to true molecular weight increases dramatically. It should also be noted that the extent of intra- and interpolymer hydrogen bonding is very sensitive to the properties of the solvent.

Recently, Lee et al.[8] reported on the high pressure cloud-point behavior of poly(ethylene-*co*-acrylic acid) (EAA) in low molecular weight hydrocarbon solvents. Although the study by Lee and co-workers[8] was primarily focused on the impact of solvent quality and copolymer acid content on the phase behavior, they showed that acid content has a larger effect on the location of the cloud-point curve than does copolymer molecular weight. Interestingly, Lee and co-workers[8] found that the cloud-point curves in slightly polar butene ordered with respect to the number average molecular weight (M_n) rather than the weight average molecular weight (M_w). In a similar study, Meilchen, Hasch, and McHugh[9] also showed that the location of the cloud-point curves of the poly(ethylene-*co*-methyl acrylate) (EMA)–monochlorodifluoromethane (CDFM) system was more sensitive to the methyl acrylate

* To whom correspondence should be sent.
® Abstract published in *Advance ACS Abstracts*, July 15, 1994.

0024-9297/94/2227-4652$04.50/0

Table 1. Physical Properties of Polyethylene, Poly(ethylene-*co*-methyl acrylate), and Poly(ethylene-*co*-acrylic acid) Used in This Study[a]

polymer	comonomer content (mol %)	crystallinity (%)	M_n	M_w	M_w/M_n
PE_{parent}	0.0	36.8	20 100	108 000	5.37
PE_A	0.0		52 100	64 800	1.24
PE_B	0.0	36.5	90 200	113 000	1.25
EMA_{parent}	35.9	0.0	33 000	108 900	3.30
EMA_A	34.6		49 200	68 900	1.40
EMA_B	34.6		93 000	112 100	1.21
EMA_C			213 800	277 900	1.30
EAA_{parent}	4.1	37.0	16 900	100 500	5.95
EAA_A	4.1	35.9	13 800	24 300	1.76
EAA_B	4.0		41 800	54 500	1.30
EAA_C	4.0	30.4	132 200	247 200	1.87

[a] The molecular weights of poly(ethylene-*co*-methyl acrylate) are based on polystyrene standards and are not corrected for long-chain branching. The molecular weights of poly(ethylene-*co*-acrylic acid) are based on polyethylene standards and are corrected for the acid content of the copolymer.

Table 2. Physical Properties of the Solvents Used in This Study[20,21]

solvent	critical temp (°C)	critical pressure (bar)	critical dens (g/cm³)	polarizability $\times 10^{25}$ (cm³)	dipole moment (debye)
butane	152.1	38.0	0.228	81.4	0.0
butene	146.4	39.7	0.234	82.4	0.4
dimethyl ether	126.8	53.0	0.258	52.2	1.3

content rather than the copolymer molecular weight. CDFM, which does not self-associate, is expected to hydrogen bond to the basic acrylate groups of the copolymer. Meilchen found that the cloud-point curves of EMA–CDFM ordered with respect to M_w, not M_n.

In this paper, data are presented on the effect of molecular weight on the cloud-point behavior of the polyethylene (PE)–dimethyl ether (DME) and EMA–butane systems to further investigate whether the location of the cloud-point curve depends on M_w or M_n. These results are compared with those for the previously reported EAA–butene system.[8] PE[9] and EMA[10,11] were fractionated using supercritical fluid solvent techniques to obtain samples of narrow molecular weight, polydispersity, and chemical composition, as shown in Table 1.

Table 2 lists the solvents used in this study along with selected physico-chemical properties that provide some insight into the energetic interactions that are in operation with each of the polymer–solvent mixtures. With nonpolar PE–solvent systems, the polarizability and density of the solvent are expected to have a large impact on the location of the cloud-point curve.[12] However, it is shown that for the PE–DME system, the polarity of DME is found to have a dominant effect on the shape of the cloud-point curve in pressure–temperature space especially at low to moderate temperatures.[8] For the EMA–butane system, strong polar interactions between acrylate groups in the backbone of the copolymer fix the shape of the cloud-point curve, again, especially at low to moderate temperatures.[10] For the EAA–butene system, in which both the copolymer and solvent are slightly polar, the dominant interaction is the dimerization of the acrylic acid groups in the backbone of the copolymer at temperatures below ~160 °C.[8] Butene also is expected to form weak π-complexes with the acid repeat units in the copolymer which enhances copolymer solubility.[8] The data generated in this study are modeled with the SAFT equation of state[13–17] to determine whether this equation, developed especially for mixtures that exhibit hydrogen bonding or complex formation, accounts for the effect of molecular weight.

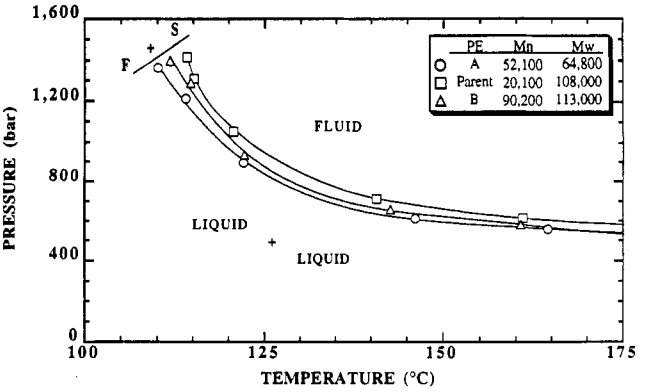

Figure 2. Effect of molecular weight on the cloud-point curves for polyethylene–dimethyl ether mixtures measured in this study.

Experimental Section

The cloud-point curves presented here are obtained using a high-pressure, variable-volume cell that is described in detail elsewhere.[8,9] Cloud-point pressures, measured at a fixed copolymer concentration of ~5 wt %, the expected maximum in the pressure–composition curves,[8,18] are reproducible to ±5 bar at temperatures above ~140 °C and ±10 bar at lower temperatures. The DuPont Corp. kindly donated the polyethylene and the ethylene–methyl acrylate copolymer. Butane, 1-butene, and dimethyl ether (all CP grade, 99.0% minimum purity) were obtained from MG Industries and were used as received.

Results and Discussion

Figure 2 shows the effect of molecular weight on the cloud-point behavior of polyethylene (PE) in polar dimethyl ether. The cloud-point curves shown in Figure 2 are terminated at the crystallization boundaries of PE. The shapes of the cloud-point curves are characteristic of upper critical solution temperature (UCST) behavior. At temperatures greater than 140 °C the cloud-point curves for the parent PE and the fractions are essentially flat, but they increase slowly in pressure as the temperature is lowered. The UCST behavior is a result of enhanced polar DME–DME interactions that are expected to increase inversely with temperature. All of the PE–DME cloud-point curves are nearly parallel over the entire temperature range shown in the figure. At low temperatures the curves order with respect to M_w, although at high pressures there is only a ~5-deg difference in temperature between the lowest and highest M_w cloud-point curves. At a fixed temperature of 115 °C, the maximum difference in cloud-point pressures between the curves is about 200 bar. The cloud-point curve for the parent PE is located at slightly higher temperatures than the curve for PE_B, even though the M_w of PE_B is slightly higher than that of the parent. The parent material, which has a polydispersity of 5.37 compared to 1.25 for PE_B, contains a larger amount of very high molecular weight oligomers that have a significant effect on the location of the cloud-point curve.

The behavior of the PE–DME system is very similar to that of the nonpolar polymer–nonpolar solvent, PE–ethane system studied by Hasch et al.[19] Ethane has a polarizability of 45.0×10^{-25} cm³, which is less than that of DME, but ethane has no dipole or quadrupole moments.[20] Hasch and co-workers found that the PE–ethane cloud-point curves varied only slightly in pressure from 120 to 150 °C, suggesting that the phase behavior is fixed by temperature-independent dispersion forces. The maximum difference in cloud-point pressures between the curves was about

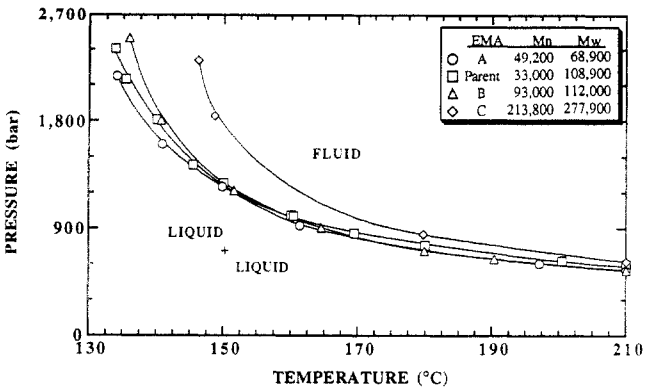

Figure 3. Effect of molecular weight on the cloud-point curves for poly(ethylene-*co*-methyl acrylate)–butane mixtures measured in this study. This copolymer contains ~35 mol % methyl acrylate.

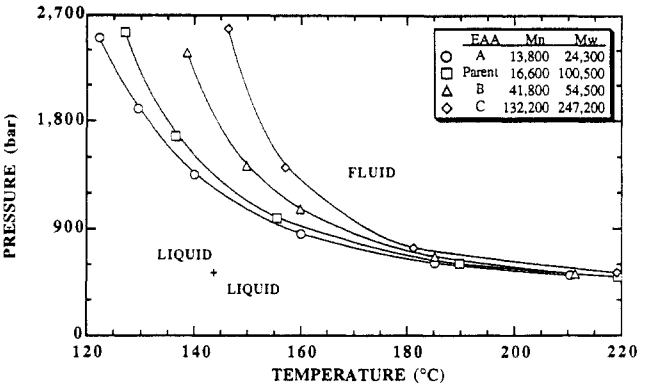

Figure 4. Effect of molecular weight on the cloud-point curves for poly(ethylene-*co*-acrylic acid)–butene mixtures.[8] This copolymer contains ~4.1 mol % acrylic acid.

200 bar, and the curves increase in pressure with respect to M_w, similar to the behavior of the PE–DME system. Irani and Cozewith also showed that the cloud-point curves for the poly(ethylene-*co*-propylene)–hexane system, another nonpolar polymer–nonpolar solvent system, also order with respect to M_w, not M_n.[18]

The poly(ethylene-*co*-methyl acrylate) (EMA)–butane system is chosen to determine the effect of molecular weight on the cloud-point curves for a polar polymer in a nonpolar solvent. The backbone of this copolymer contains 35 mol % polar methyl acrylate, which has a polarizability of 87.9×10^{-25} cm^3 and a dipole moment of 1.7 debye, and 65 mol % nonpolar ethylene, which has a polarizability of 42.3×10^{-25} cm^3. Figure 3 shows the effect of molecular weight on the cloud-point curves for EMA in nonpolar butane. The cloud-point curves exhibit UCST behavior at temperatures below 150 °C. Since butane is nonpolar, it is reasonable to attribute the increase in the cloud-point pressure with decreasing temperature to increased polar interactions between methyl acrylate repeat units. Although this EMA copolymer is very polar, the cloud-point curves order with respect to M_w as they did for nonpolar PE in DME and ethane. For M_w up to ~120 000, two characteristics of the EMA–butane system are very similar to those of the PE–DME system. A 5-deg spread was observed in cloud-point temperatures at high pressures and a 200-bar difference was observed between the EMA–butane curves with M_w of 112 000 and 68 900.

Meilchen et al.,[9] who worked with essentially the same EMA copolymer, showed that the cloud-point curves of the EMA–chlorodifluoromethane (CDFM) system that exhibits LCST behavior also order with respect to M_w. CDFM, a proton donor, is expected to hydrogen bond to the acrylate group, a proton acceptor, but CDFM does not self-associate. The EMA–CDFM data demonstrate that even though interpolymer hydrogen bonding occurs between the polymer and the solvent, the cloud-point curves still order with respect to M_w.

Figure 4 shows the effect of molecular weight on the cloud-point behavior of the poly(ethylene-*co*-acrylic acid) (EAA)–butene mixtures obtained by Lee and co-workers.[8] The backbone of this copolymer contains 4.1 mol % polar acrylic acid, which has a polarizability of 87.9×10^{-25} cm^3 and a dipole moment of 1.7 debye, and 95.9 mol % nonpolar ethylene, which has a polarizability of 42.3×10^{-25} cm^3. As the temperature increases above 180 °C, the EAA–butene cloud-point curves exhibit behavior that is similar to that of the PE–ethane system, suggesting that EAA and butene interact predominantly by dispersion forces and that the amount of acid dimerization is reduced.[1,3] It is difficult to determine whether the cloud-point pressures order with respect to M_w or M_n because the cloud-point curves are so closely grouped together at high temperatures. However, as the temperature decreases below 180 °C, the cloud-point curves increase dramatically in pressure and they diverge from one another. On the basis of the characteristics of the PE–DME and EMA–butane systems, the differentiation of the EAA–butene curves at low temperatures is attributed to hydrogen bonding between acrylic acid repeat units. In contrast to the other systems reported here, the cloud-point curves for the EAA–butene system order with respect to M_n at low temperatures. The divergence of these curves is much more dramatic than that observed for the two previously described systems. For example, the spread in cloud-point temperatures at high pressures is as much as 3 times that of the PE–DME or the EMA–butane systems. Also, the maximum difference in cloud-point pressures between the EAA–butene curves is 600–1200 bar, which is 3–6 times that for the PE–DME or the EMA–butane systems. The ordering of the acid copolymer curves with M_n is a result of intrapolymer hydrogen bonding that depends on the number of acid groups rather than on their weight. The intrapolymer hydrogen bonding is so strong that the addition of only 4.1 mol % acrylic acid repeat unit in the backbone structure switches the ordering of the location of cloud-point curves from M_w to M_n. The work of Meilchen et al. for the EMA–CDFM system[9] suggests that the acid copolymer curves would order by M_w if the intermolecular hydrogen bonding predominated. Note that the curve for the polydisperse parent EAA ($M_w/M_n = 5.95$) is only slightly shifted from that for EAA$_A$ ($M_w/M_n = 1.98$), suggesting that molecular weight polydispersity only has a secondary effect on the location of the acid cloud-point curves.

Modeling

Statistical associating fluid theory (SAFT) is used to model the molecular weight-dependent phase behavior exhibited by the polymer–solvent mixtures reported in this paper. The objective of this modeling is to determine whether SAFT can predict the effect of polymer molecular weight on the phase behavior. The SAFT equation is developed from expressions for the residual Helmholtz free energy, a^{res}, given by

$$a^{res} = (a^{hs} + a^{chain} + a^{assoc}) + a^{disp} \quad (1)$$

The a^{hs} term, developed by Carnahan and Starling,[22] accounts for segment–segment hard-sphere repulsive interactions; the a^{chain} term, derived by Chapman,[13] accounts for the covalent bonds that exist between

Table 3. Pure Component Parameters for *n*-Butane, 1-Butene, and Dimethyl Ether Used with the SAFT Equation[25]

component	v^{00} (cm³/mol)	m	u^0/k (K)	ϵ/k (K)	v (cm³/mol)
n-butane	12.599	3.458	195.11	0	0
1-butene	13.154	3.162	202.49	0[a]	0[a]
dimethyl ether	11.536	2.799	207.83	0[a]	0[a]

[a] Does not self-associate, but is able to form complexes with acrylic acid groups.

Table 4. Pure Component Parameters for Polyethylene, Poly(ethylene-*co*-methyl acrylate), and Poly(ethylene-*co*-acrylic acid) Used in This Study with the SAFT Equation

polymer	v^{00} (cm³/mol)	m	u^0/k (K)	ϵ/k (K)	v (cm³/mol)
PE_{parent}	12.000	1024.3	216.15	0	0
PE_A	12.000	2655.0	216.15	0	0
PE_B	12.000	4596.6	216.15	0	0
EMA_{parent}	12.216	1560.9	220.00	0	0
EMA_A	12.216	2327.2	220.00	0	0
EMA_B	12.216	4398.9	220.00	0	0
EMA_C	12.216	10113.0	220.00	0	0
EAA_{parent}	12.000	861.3	216.15	5787	0.0339
EAA_A	12.000	703.3	216.15	5787	0.0339
EAA_B	12.000	2130.2	216.15	5787	0.0339
EAA_C	12.000	6737.2	216.15	5787	0.0339

segments of the molecule; and the a^{assoc} term, also derived by Chapman,[13] is based on the associating fluid theory of Wertheim[23-26] developed to account for the formation of association at specific sites on the molecule. The sum of these three terms comprise the reference equation used in SAFT. The a^{disp} term, derived by Alder,[27] represents a perturbation from the reference equation accounting for mean-field dispersion and induction interactions. Details on the explicit expressions used for the terms in eq 1 can be found elsewhere and are not reproduced here.[13-17]

The expression for the residual Helmholtz free energy is used, along with thermodynamic definitions, to derive an equation for the fugacity coefficient, ϕ_i, used to calculate phase equilibria

$$\ln \phi_i = \frac{\mu_i^{res}}{RT} - \ln Z \tag{2}$$

where Z is the compressibility of the mixture, R is the gas constant, T is the temperature, and μ_i^{res} is the residual chemical potential. The residual chemical potential is defined as

$$\frac{\mu_i^{res}}{RT} = \left(\frac{\partial(Na^{res}/RT)}{\partial N_i}\right)_{T,V,N_{j\neq i}} \tag{3}$$

where N is the total number of moles in the system, N_i represents the number of moles of component i in the system, and V is the total mixture volume. Equation 2 can be rewritten in terms of the residual Helmholtz energy as

$$\ln \phi_i = \left\{\frac{\partial[a^{res}/RT]}{\partial x_i}\right\}_{T,V,N_{j\neq i}} - \sum x_j \left\{\frac{\partial[a^{res}/RT]}{\partial x_j}\right\}_{T,V,N_{j\neq i}} + a^{res}/RT + (Z-1) - \ln Z \tag{4}$$

where x_i is the mole fraction of component i. The derivatives in eq 4 are given in a parameterized form by Huang and Radosz.[16] It should be noted that eq A24 in Huang and Radosz is in error and has been subsequently corrected.[17]

In the SAFT equation, there are five pure-component parameters: v^{00}, the temperature-independent volume of a segment; u^0/k, the temperature-independent energy parameter for attraction between two segments; m, the number of segments in a molecule; e^{AB}, the energy of association between sites on a molecule; and v^{AB}, the volume of association. The parameters e^{AB} and v^{AB} are nonzero only for hydrogen-bonding molecules. For the mixtures, three mixing rules are required: v^0, the temperature-dependent volume of a segment; u, the temperature-dependent energy of attraction between two segments; and m, the average segment size for the mixture. The mixing rule for the volume of a segment is

$$v^0 = \sum_i \sum_j x_i x_j m_i m_j v_{ij}^0 \tag{5}$$

where

$$v_{ij}^0 = \frac{1}{8}[v_i^{0\,1/3} + v_j^{0\,1/3}]^3 \tag{6}$$

and x_i is the mole fraction of component i. The mixing rule for the energy of attraction between segments is

$$\frac{u}{kT} = \frac{1}{v^0} \sum_i \sum_j x_i x_j m_i m_j \left[\frac{u_{ij}}{kT}\right] v_{ij}^0 \tag{7}$$

where

$$u_{ij} = (u_{ii}u_{jj})^{1/2}(1 - k_{ij}) \tag{8}$$

and k_{ij} is an adjustable binary mixture parameter. The average segment size for the mixture is

$$m = \sum_i \sum_j x_i x_j m_{ij} \tag{9}$$

where

$$m_{ij} = \frac{1}{2}(m_i + m_j)(1 - \eta_{ij}) \tag{10}$$

and η_{ij} is an adjustable binary mixture parameter. The effect of the two adjustable parameters is mentioned later in this paper.

Table 3 shows the pure component parameters of the solvents used in this study. The values of v^{00}, u^0/k, and m are given by Huang and Radosz[15] for butane, 1-butene, and dimethyl ether. Table 4 lists the pure component parameters for polyethylene and the two copolymers used in this study. Typically, SAFT is fit to pure component pressure–volume–temperature (PVT) data to determine values for v^{00}, u^0/k, and m. Since EAA contains only ~4.0 mol % acrylic acid, v^{00} and u^0/k are set equal to the values used for polyethylene. The number of segments of EAA is determined by the correlation developed for polyalkenes relating the segment number to the polymer molar mass. The energy of acrylic acid association, ϵ^{AA}/k, is determined from spectroscopic measurements reported by Otocka and Kwei[3] for EAA. They find that the enthalpy of hydrogen bond formation is equal to 11.5 kcal/mol of dimer, which, when divided by the gas constant, gives a value of 5787 K for ϵ^{AA}/k. Although this energy of dimerization is quite

large, it should be noted that two bonds are formed when acrylic acid dimerizes. It is difficult to unequivocally determine a value for v^{AA}, the volume of dimerization of the acid groups in the backbone of the copolymer, since there is only a small amount of data availablie for these copolymers. In this study v^{AA} is fixed at 0.0339 cm^3/mol, which is similar to the values found by Radosz and Huang[15] when fitting SAFT to pure component data for low molecular weight carboxylic acids.

Since, to the best of our knowledge, there are no acid–alkene spectroscopic data available in the literature, the values of ϵ^{AB}/k are estimated by analogy to available alcohol–alkene data. Van Ness and co-workers[28] report that the energy of alcohol–alcohol hydrogen bonding decreases by 38% when toluene, rather than heptane, is used as the background solvent. Therefore, ϵ^{AB}/k is set equal to 2225 K, which is 38% of ϵ^{AA}/k.

It is not possible to substitute polyethylene pure component parameters for the EMA copolymer used in this study since this copolymer contains 35 mol % methyl acrylate. Therefore, EMA pure component parameters are calculated using an approach suggested by Panayiotou[29] which treats the parameters of the copolymer as weighted averages of the two homopolymers, polyethylene and poly(methyl acrylate) (PMA). Since there are no PVT data available for PMA, poly(vinyl acetate) data[30] are used to simulate PMA. Also, for these calculations, the copolymer is assumed to be statistically random. The temperature-independent volume of a segment of EMA, v^{00}_{co}, is calculated by assuming pairwise additivity of the segment volumes for the two homopolymers which comprise the copolymer.

$$v^{00}_{co} = \sum_{A=1}^{2}\sum_{B=1}^{2} x_A x_B v^{00}_{AB} \tag{11}$$

where

$$v^{00}_{AB} = 0.5[(v^{00}_{AA} + v^{00}_{BB})(1 - \eta_{AB})] \tag{12}$$

The subscripts A and B represent the two monomers in the copolymer and x_A and x_B represent their mole fractions in the copolymer. The temperature-independent energy of the copolymer, u^0_{co}, is determined using a van der Waals-type mixing rule

$$u^0_{co} = \frac{1}{v^{00}_{co}} \sum_{A=1}^{2}\sum_{B=1}^{2} x_A x_B u^0_{AB} v^{00}_{AB} \tag{13}$$

where

$$u^0_{AB} = (u^0_{AA} u^0_{BB})^{0.5}(1 - k_{AB}) \tag{14}$$

and u^0_{AA} and u^0_{BB} represent the temperature-independent energy of homopolymers A and B. Two adjustable copolymer mixture parameters, k_{AB} and η_{AB}, are used to account for specific interactions between the two homopolymers, A and B, which comprise the copolymer. However, these parameters are set equal to zero in this study. The mixing rule for the number of segments a pure copolymer occupies, m_{co}, is given by

$$m_{co} = \sum_{A=1}^{2}\sum_{B=1}^{2} x_A x_B m_{AB} \tag{15}$$

where

$$m_{AB} = 0.5(m_{AB} + m_{BB}) \tag{16}$$

and m_{AA} and m_{AA} represent the number of segments of homopolymers A and B, respectively.

Although it is recognized that the molecular weight distribution can have a large effect on the location of the cloud-point curve,[31-33] the distribution of the parent material is neglected since our objective is to determine whether SAFT can capture the effect of molecular weight rather than polydispersity. The calculated cloud-points are obtained by generating pressure–composition isotherms at various temperatures and selecting the pressures at which each isotherm intersects a composition equal to 5 wt % polymer. To simplify the calculations, the assumption is made that the acid sites along the backbone of any particular oligomer are equivalent regardless of the adjacency of the acid groups. As shown in Huang and Radosz, the equations that relate the contribution of hydrogen bonding to SAFT involve summations over the different sites. In this work, summations taken over the different sites on an EAA oligomer are replaced by summations over the different *types* of sites multiplied by the number of equivalent sites. Knowing the number average molecular weight and chemical composition of EAA, the number of equivalent sites is readily calculated.

Figure 5 shows the result of the SAFT calculation for three different samples of polyethylene in dimethyl ether. The value of the binary mixture parameter, k_{ij} = 0.0405, is determined by the best fit of the SAFT equation to the cloud-point curve of the parent PE–DME mixture. The other binary mixture, η_{ij}, is set equal to zero for these calculations. These values of the mixture parameters are used to calculate the cloud-point curves for the two PE samples that have number average molecular weights of 52 100 and 90 200. SAFT predicts the correct trend observed for the effect of molecular weight on the phase behavior at temperatures near 125 °C, although the predictions are not quantitative. SAFT overpredicts by about 1 order of magnitude the increase in cloud-point temperature with increasing M_w going from 65 000 to 108 000. However, SAFT does correctly show that the increase in cloud-point temperature diminishes as M_w is increased further to 113 000. The poor performance of SAFT in this instance is not entirely unexpected since it takes a rather large value of k_{ij} to fit the parent cloud-point curve. The poor performance of SAFT is also more than likely a result of the equation not accounting for the polar interactions between DME molecules. Walsh, Guedes, and Gubbins[34] have recently reported on a modified version of SAFT that specifically accounts for polarity. Calculations with this modified version of SAFT will be investigated in the near future.

As mentioned previously, the pure component parameters for EMA are determined from mole fraction weighted averages of the parameters of PE and poly(vinyl acetate). With this approach v^{00} is equal to 12.216 and u^0/k is equal to 248 K for EMA. Figure 6 shows the effect of k_{ij} on the calculated cloud-point curve for the parent EMA–butane mixture. For these calculations η_{ij} is set equal to zero. With k_{ij} less than 0.015, the calculated cloud-point curves remain flat to temperatures as low as 130 °C, whereas the experimental cloud-point data increase rapidly in pressure at temperatures near 160 °C. With k_{ij} equal to 0.015 the calculated cloud-point curve has the same characteristic shape as the experimental curve, although it is shifted by about 1000 bar to higher pressures. Also, increasing the value of k_{ij} has a larger impact on the shape and location of the cloud-point curve at temperatures near 135 °C than it does at temperatures above 200 °C.

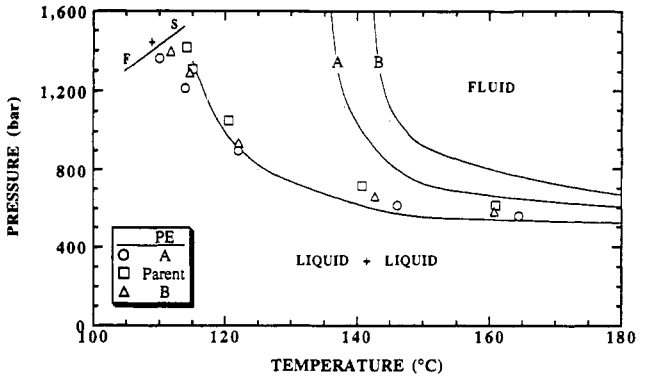

Figure 5. Comparison of experimental and calculated cloud-point curves for PE_{parent}, PE_A, and PE_B in dimethyl ether. For these calculations $k_{ij} = 0.0405$ and $\eta_{ij} = 0.0$.

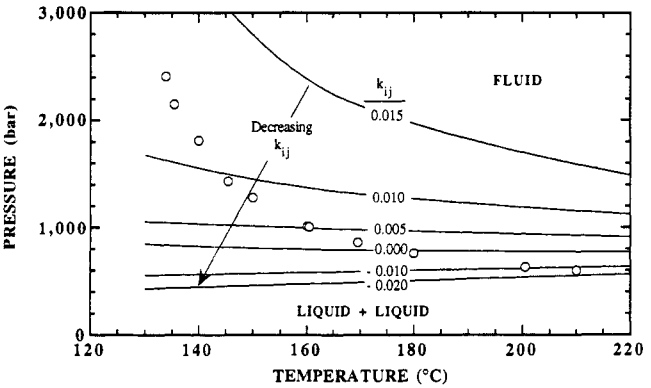

Figure 6. Effect of k_{ij} on the location of cloud-point curves calculated with the SAFT equation of state for the parent EMA–butane mixture. The open circles represents experimental cloud-point data for the parent EMA–butane mixture. For these calculations u^0_{co}/k and η_{ij} are 248 K and 0.0, respectively.

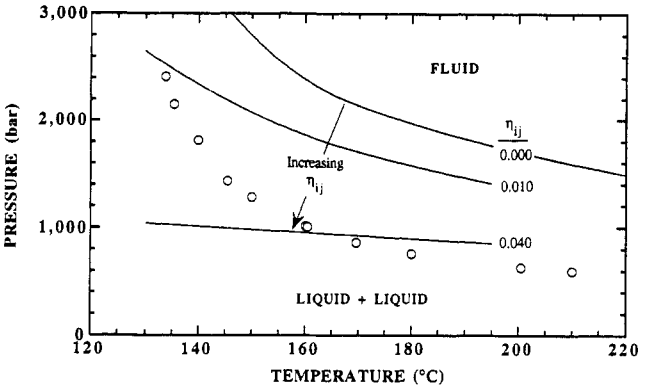

Figure 7. Effect of η_{ij} on the location of cloud-point curves calculated with the SAFT equation of state for the parent EMA–butane mixture. The open circles represent experimental cloud-point data for the parent EMA–butane mixture. For these calculations u^0_{co}/k and k_{ij} are 248 K and 0.015, respectively.

Figure 7 shows the effect of η_{ij} on the calculations for the parent EMA–butane mixture with $u^0_{co}/k = 248$ K and $k_{ij} = 0.015$. Contrary to the effect of k_{ij}, the calculated cloud-point pressures decrease with increasing η_{ij} and the slopes of the curves decrease considerably in the low-temperature region of the graph. Even if both k_{ij} and η_{ij} are varied, it is still not possible to obtain a reasonable representation of the cloud-point curve. The poor performance of SAFT could be a consequence of the estimated values used for the pure component parameters of EMA, especially since *PVT* data for poly(vinyl acetate) are used instead of data for poly(methyl acrylate). Therefore, it is reasonable to determine the fit of SAFT with modified

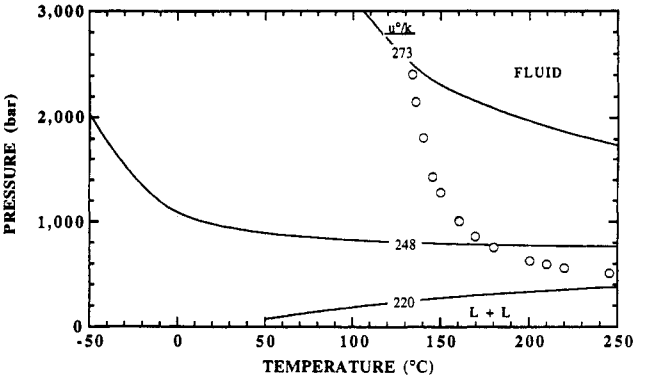

Figure 8. Effect of the temperature-independent energy parameter on the location of cloud-point curves calculated with the SAFT equation of state for the parent EMA–butane mixture. The open circles represent experimental cloud-point data for the parent EMA–butane mixture. For these calculations η_{ij} and k_{ij} are both set equal to zero.

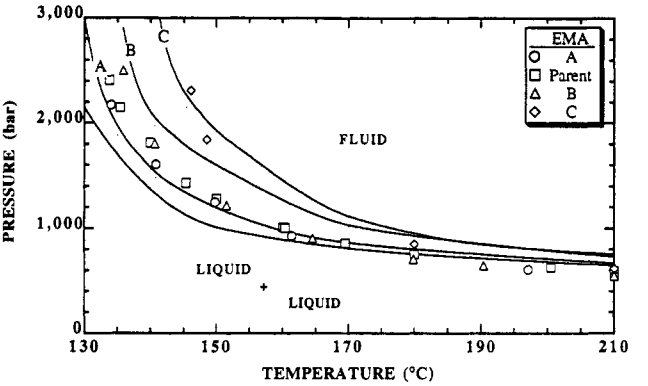

Figure 9. Comparison of experimental and calculated cloud-point curves for EMA_{parent}, EMA_A, EMA_B, and EMA_C in butane. For these calculations $k_{ij} = 0.026$, $\eta_{ij} = 0.0$, and $u^0_{co}/k = 220$ K.

values of v^{00}_{co}, u^0_{co}/k, and m. Varying v^{00}_{co} and m by as much as ±10% had less effect than u^0_{co}/k on the location of the calculated cloud-point curve. Varying u^0_{co}/k by ±10% has a large effect on the characteristics of the cloud-point curve, as shown in Figure 8. In this calculation, k_{ij} and η_{ij} are both set to zero. The calculated cloud-point pressures for $u^0_{co}/k = 248$ K remain essentially constant until the temperature is lowered below 0 °C, whereas the experimental cloud-point pressures begin to increase rapidly near 160 °C. With u^0_{co}/k set equal to 273 K, the calculated cloud-point pressures increase more slowly with decreasing temperature, but the curve is located at much higher pressures. Decreasing the value of u^0_{co}/k to 220 K causes the calculated cloud-point curve to shift to very low pressures and to exhibit a slight positive slope. A compromise is needed in the values of u^0_{co}/k, k_{ij}, and η_{ij} to obtain a reasonable fit of the EMA–butene system. On the basis of the results shown in Figures 6–8, u^0_{co}/k is set equal to 220 K since it is possible to greatly increase the calculated cloud-point pressures in the low-temperature region of the diagram with a positive value of k_{ij}.

Figure 9 shows the SAFT prediction of cloud-point curves of EMA–butane mixtures using k_{ij} set equal to 0.026, η_{ij} equal to zero, and u^0_{co}/k equal to 220 K. A much closer fit of the experimental data is obtained for the EMA–butane system than was obtained for the PE–DME system. Although the proper molecular weight dependence EMA–butane system is predicted by the SAFT equation, it is not possible to determine unequivocally whether this is merely a consequence of aggressive curve fitting since u^0_{co}/k was varied over a wide range to obtain the fit. Pure

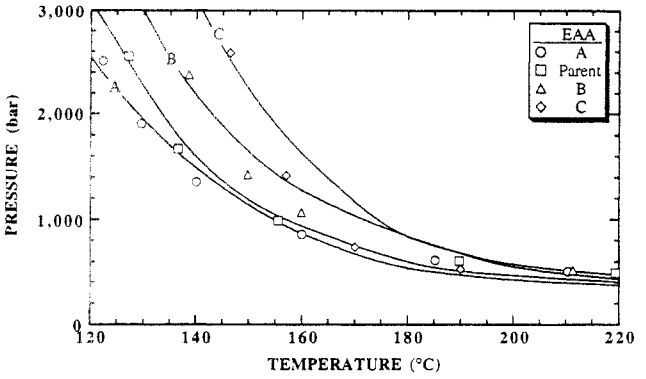

Figure 10. Comparison of experimental and calculated cloud-point curves for EAA_{parent}, EAA_A, EAA_B, and EAA_C in 1-butene. For these calculations $k_{ij} = -0.020$ and $\eta_{ij} = 0.0$.

component *PVT* data for EMA are needed to resolve this issue.

Figure 10 shows the calculation of the cloud-point curves for the EAA–butene system with k_{ij} equal to −0.020 and η_{ij} set equal to zero. In this calculation, the dispersion energy and segmental volume of EAA are set equal to the values for polyethylene. The calculated EAA–butene cloud-point curves are in very good agreement with experimental observation. For this system, the dimerization of acrylic acid segments is expected to be the dominant type of interaction at low temperatures since the energy of hydrogen bonding is roughly 1 order of magnitude larger than that expected for dispersion interactions.[35] As shown in Figure 10, SAFT properly accounts for hydrogen-bonding interactions and it can account for molecular weight effects with a small, constant value of k_{ij}. However, it should be noted that the version of SAFT used in this study does not distinguish between intra- and interpolymer hydrogen bonding.

Conclusion

The cloud-point curves for the PE–DME and EMA–butane systems both exhibit UCST-like behavior as the temperature is decreased below ~150 °C. The shapes of these curves are a consequence of strong polar interactions between solvent molecules in the PE–DME case and between copolymer oligomers in the EMA–butane case. The cloud-point curves of the EAA–butene system also exhibit UCST-like behavior at low temperatures as a consequence of acrylic acid dimerization. However, the curves for the EAA–butene system order with respect to M_n rather than M_w, as was found for the other two systems. The ordering of the EAA–butene cloud-point curves with M_n is a result of intrapolymer hydrogen bonding that depends on the number of acid groups rather than on their weight.

The SAFT equation successfully captures the characteristics of the cloud-point curves for all three systems presented in this study. However, the calculated curves for the PE–DME system are only in qualitative agreement with experimental data probably because SAFT does not properly account for polar interactions between DME molecules. For both copolymers, it is necessary to estimate pure component parameters which introduces uncertainty in the calculated results. Nevertheless, with a single mixture parameter it is possible to calculate cloud-point curves for the copolymer–solvent systems that are in very good agreement with experimental data.

Acknowledgment. The authors acknowledge the National Science Foundation for partial support of this project under Grant CTS-9122003.

References and Notes

(1) Earnest, T. R., Jr.; MacKnight, W. J. *Macromolecules* **1980**, *13*, 844.
(2) MacKnight, W. J.; Taggart, W. P.; McKenna, L. *J. Polym. Sci.* **1974**, *46*, 83.
(3) Otocka, E. P.; Kwei, T. K. *Macromolecules* **1968**, *1*, 244.
(4) Pimentel, G.; McClellan, A. *The Hydrogen Bond*; W. H. Freeman and Co.: San Francisco, **1960**; Appendix B.
(5) Longworth, R.; Morawetz, H. *J. Polym. Sci.* **1958**, *29*, 307.
(6) Chang, S. Y.; Morawetz, H. *J. Phys. Chem.* **1956**, *60*, 782.
(7) Morawetz, H.; Gobran, R. H. *J. Polym. Sci.* **1954**, *12*, 133.
(8) Lee, S.-H.; LoStracco, M. A.; Hasch, B. M.; McHugh, M. A. *J. Phys. Chem.* **1994**, *98*, 4055–4060.
(9) Meilchen, M. A.; Hasch, B. M.; McHugh, M. A. *Macromolecules* **1991**, *24*, 4874.
(10) Pratt, J. A.; Lee, S.-H.; McHugh, M. A. *J. Appl. Polym. Sci.* **1993**, *49*, 953.
(11) Pratt, J. A. M.S. Thesis, Johns Hopkins University, 1994.
(12) Hasch, B. M.; Meilchen, M. A.; Lee, S.-H.; McHugh, M. A. *J. Polym. Sci., Part B: Polym. Phys.* **1993**, *31*, 429.
(13) Chapman, W. G.; Gubbins, K. E.; Jackson, G.; Radosz, M. *Ind. Eng. Chem. Res.* **1990**, *29*, 1709–1721.
(14) Chapman, W. G.; Gubbins, K. E.; Jackson, G.; Radosz, M. *Fluid Phase Equilib.* **1989**, *52*, 31–38.
(15) Huang, S. H.; Radosz, M. *Ind. Eng. Chem. Res.* **1990**, *29*, 2284–2294.
(16) Huang, S. H.; Radosz, M. *Ind. Eng. Chem. Res.* **1991**, *30*, 1994–2005.
(17) Huang, S. H.; Radosz, M. *Ind. Eng. Chem. Res.* **1993**, *32*, 762.
(18) Irani, C. A.; Cozewith, C. *J. Appl. Polym. Sci.* **1986**, *31*, 1879.
(19) Hasch, B. M.; Lee, S.-H.; McHugh, M. A.; Watkins, J. J.; Krukonis, V. J. *Polymer* **1993**, *34*, 12, 2554.
(20) Reid, R. C.; Prausnitz, J. M.; Polling, B. E. *The properties of gases and liquids*, 4th ed.; McGraw-Hill: New York, 1987; Appendix A.
(21) David, R. L. *CRC Handbook of Chemistry and Physics*, 73rd ed.; CRC Press, 1992; Chapter 9.
(22) Carnahan, N. F.; Starling, K. E. *J. Chem. Phys.* **1969**, *51*, 635–636.
(23) Wertheim, M. S. *J. Stat. Phys.* **1984**, *35*, 19–34.
(24) Wertheim, M. S. *J. Stat. Phys.* **1984**, *35*, 35–47.
(25) Wertheim, M. S. *J. Stat. Phys.* **1986**, *42*, 459–476.
(26) Wertheim, M. S. *J. Stat. Phys.* **1986**, *42*, 477–492.
(27) Alder, B. J.; Young, D. A.; Mark, A. J. *J. Chem. Phys.* **1972**, *56*, 3013–3029.
(28) Van Ness, H. C.; Van Winkle, J.; Richtol, H. H.; Hollinger, H. B. *J. Phys. Chem.* **1967**, *71*, 1483–1494.
(29) Panayiotou, C. G. *Makromol. Chem.* **1987**, *188*, 2733.
(30) Beret, S.; Prausnitz, J. M. *Macromolecules* **1975**, *8*, 536–538.
(31) Koningsveld, R.; Staverman, A. J. *J. Polym. Sci., Polym. Phys. Ed.* **1968**, *6*, 305–323.
(32) Koningsveld, R.; Staverman, A. J. *J. Polym. Sci., Polym. Phys. Ed.* **1968**, *6*, 325–348.
(33) Koningsveld, R.; Staverman, A. J. *J. Polym. Sci., Polym. Phys. Ed.* **1968**, *6*, 349–366.
(34) Walsh, J. M.; Guedes, H. J. R.; Gubbins, K. E. *J. Phys. Chem.* **1992**, *96*, 10995–11004.
(35) Huyskens, P. L.; Luck, W. A.; Zeegers-Huyskens, T. *Intermolecular Forces, An Introduction to Modern Methods and Results*; Springer-Verlag: Berlin, 1991; Chapter 1.